EPJ Web of Conferences **69**, 00026 (2014)
DOI: 10.1051/epjconf/20146900026

Neutron to proton ratio dependence of energy of vanishing flow: role of system size and collision geometry

Sakshi Gautam[a]

[1] *Department of Physics, Dev Samaj College for Women, Sector 45B, Chandigarh-160047, India*

Abstract. We study the effects of system size on the neutron to proton ratio dependence of the energy of vanishing flow for isotopic series of various colliding nuclei. We find a significant effect of the nuclear symmetry energy on the neutron to proton ratio dependence of the energy of vanishing flow throughout the mass range for central as well as peripheral collisions. We find that the neutron to proton ratio dependence of the energy of vanishing flow for isotopic series of heavier system shows more sensitivity to the symmetry energy compared to that for lighter systems and that this sensitivity is enhanced in peripheral collisions. In addition, the mass dependence of the energy of vanishing flow has also been studied for systems having a neutron to proton ratio varying from purely symmetric matter to a highly neutron-rich one.

1 Introduction

The investigation of system size effects in various phenomena of heavy-ion collisions has attracted a lot of attention. System size dependencies have been reported for various phenomena like fusion-fission, particle production, multifragmentation, collective flow (of nucleons/fragments) as well as its disappearance, for density and temperature and so on [1–6]. Low energy fusion processes deserve a special mention, where the mass dependence was analysed using hundred of reactions. For instance, in Ref. [4] the power law scaling ($\propto A^{\tau}$) of pion/kaon production with the size of the system has been reported. A similar power law behavior for the system size dependence has also been reported for the multiplicity of various types of fragments[5]. The collective transverse in-plane flow has also been investigated extensively during the past three decades and has been found to depend strongly on the combined mass of the system [7] in addition to the incident energy [8, 9] as well as collision geometry [9]. The energy dependence of collective transverse in-plane flow has led us to its disappearance. The energy at which flow disappears has been termed as the energy of vanishing flow (EVF) [10]. The energy of vanishing flow has been found to depend strongly on the combined mass of the system [11, 12]. Similarly power law mass dependencies have also been reported for various observables in nuclear dynamics such as density, temperature, and participant-spectator matter [6].

With the advent of radioactive ion beams [13–15] the role of the isospin degree of freedom in reaction dynamics of heavy-ion collisions has been studied for the past two decade. These studies are helpful to extract information about asymmetric nuclear matter. The isospin effects in the collective transverse flow (and its disappearance) have been explained in the literature as the competition

[a] e-mail: sakshigautm@gmail.com

between various reaction mechanisms, such as nucleon-nucleon (NN) collisions, symmetry energy, the surface properties of colliding nuclei and the Coulomb force. The relative importance among these reaction mechanisms was not clear then [16]. Therefore, to get more insight about the role of the isospin degree of freedom and to explain the relative contribution of these reaction mechanisms, Gautam *et al*. have studied the EVF as a function of the combined mass of the system [17] as well as the collision geometry for isobaric pairs [18]. These studies revealed that systems with higher neutron to proton content (N/Z) have larger EVF as compared to systems with lower neutron to proton content, for all isobaric pairs in central as well as peripheral collisions. This was found to be due to the dominance of Coulomb repulsion over the symmetry energy and the isospin dependence of the NN cross-section. Since the above studies demonstrated a weaker role of the symmetry energy over the Coulomb potential for isobaric pairs, therefore, we should look at the dynamics of the energy of vanishing flow for isotopic pairs where the Coulomb potential will be same. In particular, we will study the behavior of the EVF with neutron to proton content in isotopic pairs. Moreover, since the EVF also depends significantly on the combined mass of the system, therefore, we will also look into system size effects. It thus becomes important to study the role of system size on the sensitivity of the EVF to the neutron to proton content of colliding nuclei and to see how the above predictions behave for peripheral collisions. In the present paper, our aim is, therefore, at least two fold.
(1) To study the N/Z dependence of the EVF for isotopic series throughout the mass range and range of collision geometry and to explore the role of the nuclear symmetry energy and isospin dependence of NN cross-section.
(2) To study the mass dependence of the EVF for various colliding pairs having neutron to proton ratio varying from that of pure symmetric matter to highly neutron-rich ones.
The present study will be carried out within the framework of the isospin-dependent quantum molecular dynamics (IQMD) model, the details of which can be found in Ref. [19].

2 Results and discussions

We simulated several thousands of events of the reactions of Ca+Ca, Ni+Ni, Zr+Zr, Sn+Sn, and Xe+Xe with an N/Z ratio varying from 1.0 to 2.0 in steps of 0.2. In particular, we simulated the reactions of ^{40}Ca+^{40}Ca (N/Z = 1.0), ^{44}Ca+^{44}Ca (N/Z = 1.2), ^{48}Ca+^{48}Ca (N/Z = 1.4), ^{52}Ca+^{52}Ca (N/Z = 1.6), ^{56}Ca+^{56}Ca (N/Z = 1.8), and ^{60}Ca+^{60}Ca (N/Z = 2.0); ^{56}Ni+^{56}Ni, ^{62}Ni+^{62}Ni, ^{68}Ni+^{68}Ni, ^{72}Ni+^{72}Ni, ^{78}Ni+^{78}Ni and ^{84}Ni+^{84}Ni; ^{81}Zr+^{81}Zr, ^{88}Zr+^{88}Zr, ^{96}Zr+^{96}Zr, ^{104}Zr+^{104}Zr, ^{110}Zr+^{110}Zr and ^{120}Zr+^{120}Zr; ^{100}Sn+^{100}Sn, ^{112}Sn+^{112}Sn, ^{120}Sn+^{120}Sn, ^{129}Sn+^{129}Sn, ^{140}Sn+^{140}Sn and ^{150}Sn+^{150}Sn; and ^{110}Xe+^{110}Xe, ^{120}Xe+^{120}Xe, ^{129}Xe+^{129}Xe, ^{140}Xe+^{140}Xe, ^{151}Xe+^{151}Xe and ^{162}Xe+^{162}Xe at $\hat{b}$ (b/b_{max}) = 0.2 - 0.4, 0.4 - 0.6 and 0.6 - 0.8. We used a soft equation of state along with the standard isospin- and energy-dependent cross-section reduced by 20%, i.e. $\sigma = 0.8\ \sigma_{nn}^{free}$.

To see the isospin effects, we will also discuss the EVF for all nucleons, neutrons and protons and see if the behavior of the EVF with increasing neutron content depends on the type of particle. In Fig. 1, we display the neutron to proton ratio dependence of the EVF for the isotopic series of Ca (circles), Ni (squares), Zr (triangles), Sn (diamonds) and Xe (pentagons) for central collisions of $\hat{b}$ = 0.2 - 0.4. The top, middle and bottom panels display the EVF for all nucleons, neutrons and protons, respectively. From the figure, we see that the EVF decreases with increasing neutron content for all the colliding pairs, as obtained earlier for the Ca series. This is because the increased Coulomb potential in heavier systems enhances the flow and thus, reduces the EVF. This is opposite to what has been observed for isobaric pairs (in Ref. [17]), where the EVF increases with an increase in neutron content and was attributed to the dominance of Coulomb repulsion for proton-rich colliding pairs. Moreover, the EVF decreases as we move to heavier colliding pairs from Ca+Ca to Xe+Xe. In the present case,

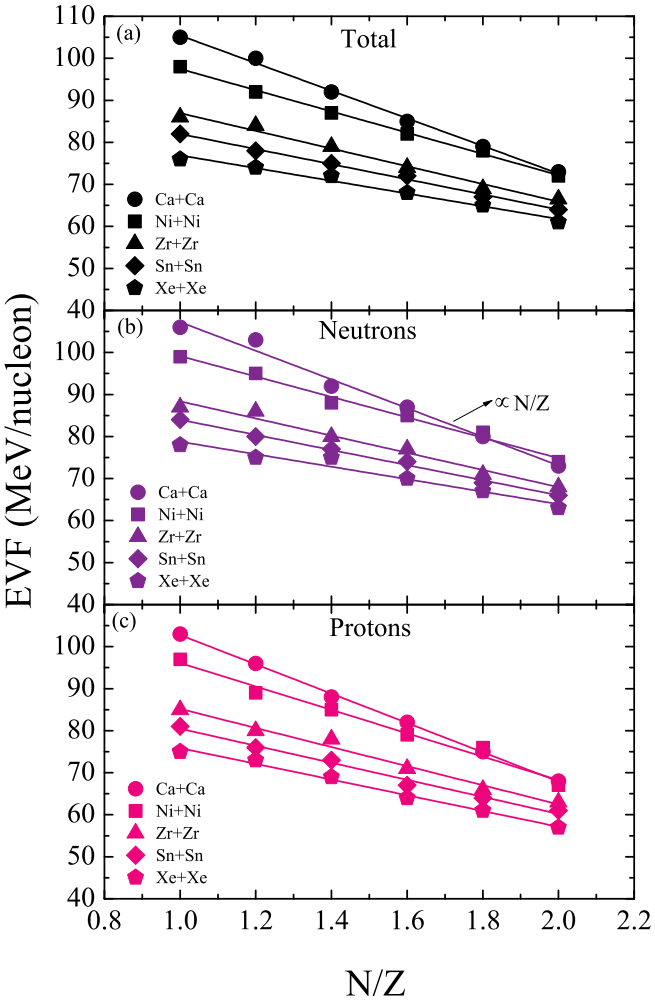

Figure 1. The EVF as a function of the N/Z ratio for the isotopic series of Ca+Ca, Ni+Ni, Zr+Zr, Sn+Sn and Xe+Xe. The top, middle and bottom panels represent the EVF for all nucleons, neutrons and protons, respectively. The lines are linear fits proportional to N/Z. Various symbols are explained in the text.

we have isotopic pairs (having the same Coulomb potential) in which the mass also increases when we move to neutron-rich systems. The decrease in the EVF with increasing neutron content thus may be either due to the increase in mass or the increased role of the symmetry energy. From the figure, we also find that the EVF follows a linear behavior ($\propto$ N/Z) with increasing neutron content of the

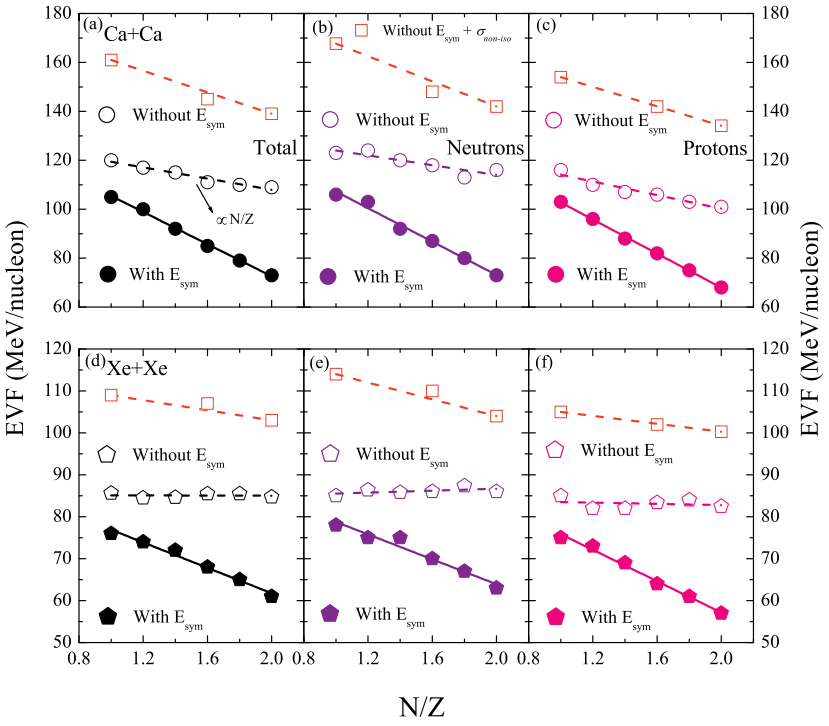

Figure 2. The N/Z dependence of the EVF for the reactions involving various isotopes of Ca (upper panels) and Xe (bottom), respectively. The results are displayed for all nucleons (left panels), neutrons (middle) and protons (right) without the symmetry energy and without the symmetry energy and with and isospin independent *NN* cross-section. The lines are linear fits proportional to N/Z. Various symbols are explained in the text.

colliding pairs for all masses. The magnitude of the slopes are 33, 25, 21, 18 and 15 for the series of Ca, Ni, Zr, Sn and Xe, respectively. We also find that the behavior of the EVF for neutrons (middle panel) and protons (bottom) is similar to that for all nucleons. The slopes are 34, 24, 20, 18 and 15 for neutrons and 35, 28, 21, 20 and 19 for protons for the Ca, Ni, Zr, Sn and Xe series, respectively. We also find that the decrease in the EVF becomes less steep with the increase in mass of the colliding pair.

2.1 Role of the symmetry energy and the isospin dependence of the nucleon-nucleon cross-section

As we have discussed earlier, the decrease in the EVF with increasing neutron content of the colliding pair may be due to either mass effects or symmetry energy effects. So to check the relative importance of these mechanisms, we calculated the EVF for two extreme masses of the Ca+Ca and Xe+Xe series

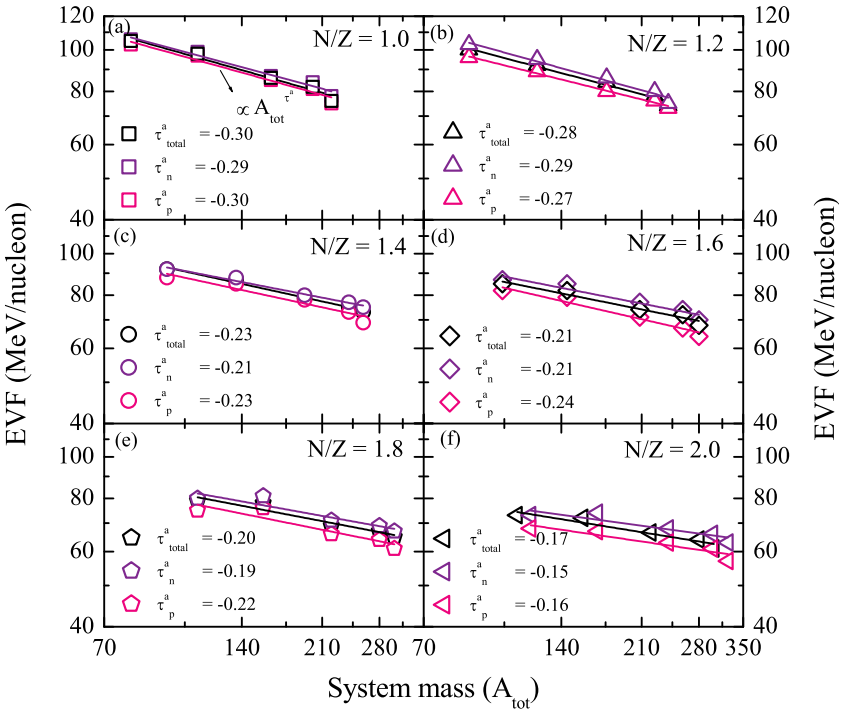

Figure 3. The EVF as a function of combined reacting mass for various N/Z ratios. The lines are power law fits $\propto A_{tot}^{\tau^a}$. The black, purple and pink symbols represent the EVF for all nucleons, neutrons and protons, respectively.

without symmetry energy. The results are displayed in Fig. 2 for the Ca+Ca (upper panels, open circles) and Xe+Xe (lower panels, open pentagons) reactions. From Fig. 2 (a) and (d), we see that on excluding the symmetry energy, the EVF increases for both the Ca and Xe series. This is because the repulsive nature of the symmetry energy leads to an increase in the flow and thus, lowers the EVF. We also see that now the behavior of the EVF with N/Z ratio is less steep with the magnitude of the slopes being 11 and 1 for the Ca and Xe series, respectively. The change in the slope is about 67 % (93 %) for the Ca (Xe) series. The slight decrease in the EVF is because of the mass effects. From this, we can conclude that the symmetry energy is dominant in lowering the EVF with increasing neutron content throughout the mass range.

Since the isospin degree of freedom also comes into the picture through the isospin dependence of the in-medium nucleon-nucleon cross section, as a next step, we also wish to check the sensitivity of the binary cross section to the N/Z dependence of the EVF. For this, we further make the binary *NN* cross section isospin independent and calculate the EVF for three masses having N/Z ratios of 1.0, 1.6 and 2.0. The results are displayed in Fig. 2 (open squares). We find that the EVF further

increases when we make the cross section isospin independent. The increase in the EVF is larger for neutron-poor systems (N/Z = 1.0) compared to neutron-rich systems (N/Z = 2.0). This is because of the fact that for systems with higher neutron content, the number of neutron-neutron and neutron-proton collision pairs increases. But the increase in the neutron-neutron collision pairs is much larger than that of the neutron-proton collision pairs. Since the probability of a neutron-neutron collisions is three times less compared to a neutron-proton collisions, the possibility of neutron-proton collisions is smaller in systems with higher neutron content.

The magnitude of slope now becomes 22 (6) for the Ca+Ca (Xe+Xe) series. The slope now changes by 33 % (60 %) for Ca+Ca (Xe+Xe) reactions. Similar behavior is exhibited by the EVF for the neutrons (Fig. 2 (b) & (e), middle panels) and protons (Fig. 2 (c) & (f), right) when we make the calculations without the symmetry energy (open circles) and without the symmetry energy and with an isospin independent *NN* cross section (open squares). The magnitude of slopes without the symmetry energy now become 10 (14) for neutrons (protons) and 26 (20) without the symmetry energy and wiht an isospin independent cross-section for the Ca+Ca series, respectively. Similarly, for Xe+Xe reactions, the magnitude of slopes become 1 (1) and 10 (5) for neutrons (protons) without the symmetry energy and without the symmetry energy and with an isospin independent *NN* cross section. From the above discussion, we have found that the change in the slope is more for heavier masses indicating that the N/Z dependence of the EVF for heavier systems can act as good probe to constrain the symmetry energy and its density dependence.

2.2 System size dependence of the EVF

In Fig. 3, we display the system size dependence of the EVF for various N/Z ratios of 1.0 (squares), 1.2 (triangles), 1.4 (circles), 1.6 (diamonds), 1.8 (pentagons) and 2.0 (left triangles). The black, purple and pink symbols represent the calculations for all nucleons, neutrons and protons, respectively. From the figure, we find that the EVF follows a power law behavior with system size ($\propto A_{tot}^{\tau^a}$) for all N/Z ratios. The power law factors τ^a for N/Z ratios of 1.0, 1.2, 1.4, 1.6, 1.8 and 2.0, are -0.30 (-0.29) [-0.30], -0.28 (-0.29) [-0.27], -0.23 (-0.21) [-0.23], -0.21 (-0.21) [-0.24], -0.20 (-0.19) [-0.22], and -0.17 (-0.15) [-0.16] for all nucleons (neutrons) [protons], respectively. Thus, we see that the power law factors are almost independent of the type of nucleons. We also see that the power law factor decreases when we go to higher N/Z ratios. This is because of the fact that, when we move to higher neutron content, the EVF of lighter systems changes drastically but the EVF of heavier systems does not change much, thus making the EVF dependence less steep for neutron-rich systems.

2.3 Impact parameter dependence of the EVF with neutron to proton ratio

From the previous discussion, we found that the behavior of the EVF with increasing neutron content is similar for all nucleons, neutrons or protons. Therefore, in the following sections, we will discuss the EVF for all nucleons only. Various studies indicate that isospin effects are found to be more pronounced in peripheral collisions [18]. So as a next step, we look at the role of the collision geometry on the N/Z dependence of the EVF. In Fig. 4, we display the N/Z dependence of the EVF for $\hat{b}$ = 0.2 - 0.4 (top panel, as in Fig. 1), 0.4 - 0.6 (middle panel) and 0.6 - 0.8 (bottom panel). From the figure, we find that at all the collision geometries the EVF follows a linear behavior with N/Z. The magnitude of the slopes are 33, 25, 21, 18, and 15 (at $\hat{b}$ = 0.2 - 0.4); 58, 41, 27, 19, and 18 (at $\hat{b}$ = 0.4 - 0.6) and 187, 115, 67, 39, and 36 (at $\hat{b}$ = 0.6 - 0.8) for the series of Ca, Ni, Zr, Xe and Sn isotopes, respectively. From the figure, we also find that
(i) the N/Z dependence of the EVF is steeper for the lighter systems compared to the heavier systems

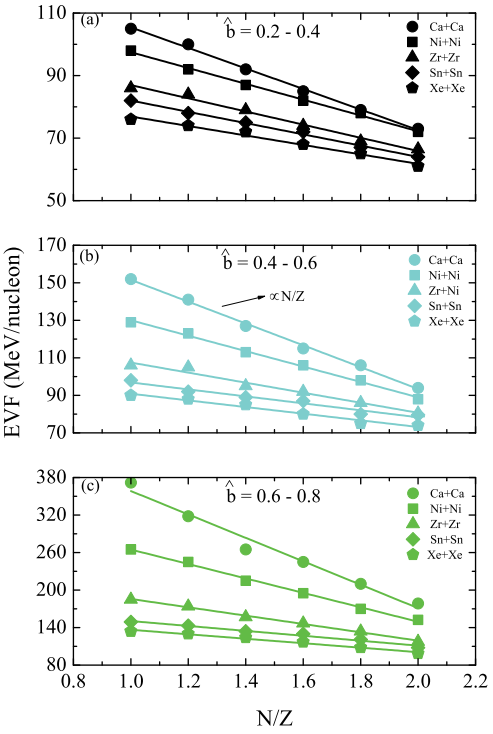

Figure 4. The EVF as function of the N/Z ratio for reactions involving various isotopes of Ca, Ni, Zr, Sn and Xe at $\hat{b}$ = 0.2 - 0.4 (top panel), 0.4 - 0.6 (middle) and 0.6 - 0.8 (bottom). The symbols have the same meaning as in Fig. 1. The lines are linear fits proportional to N/Z.

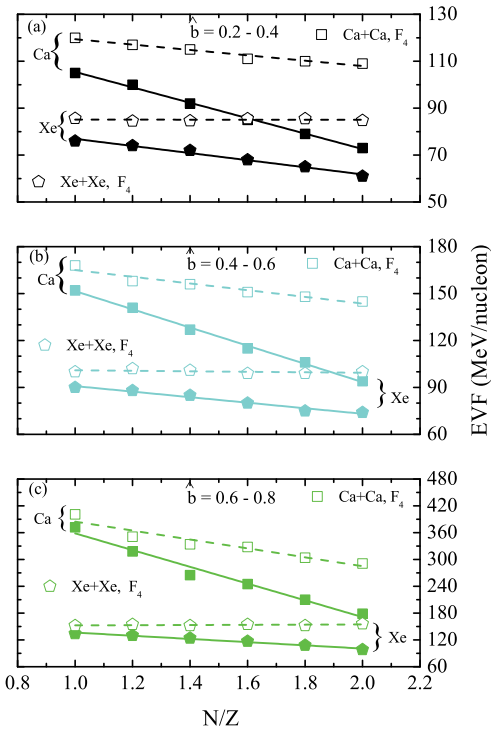

Figure 5. The EVF as a function of the N/Z ratio for reactions involving various isotopes of Ca and Xe without the symmetry energy (open symbols). The closed symbols represent calculations with the symmetry energy.

independent of the collision geometry,
(ii) for a particular isotopic series, the slope of the N/Z dependence of the EVF is larger for a peripheral collision geometry.
(iii) and the change in slope is larger for lighter systems as compared to the heavier systems when we move from central to peripheral collision geometries.
From the figure, we see that for the Ca series, the slope increases by almost 400% when we move from central to peripheral collisions, whereas for the Xe series the increase in the slope is almost 150%. We have discussed that the N/Z dependence of the EVF is sensitive to the symmetry energy and is insensitive to the isospin dependence of the *NN* binary cross section. Also, the decrease in the EVF with an increase in the N/Z ratio is due to the enhanced role of the repulsive symmetry energy for higher N/Z ratios. As we have discussed the role of the symmetry energy for central collisions, here

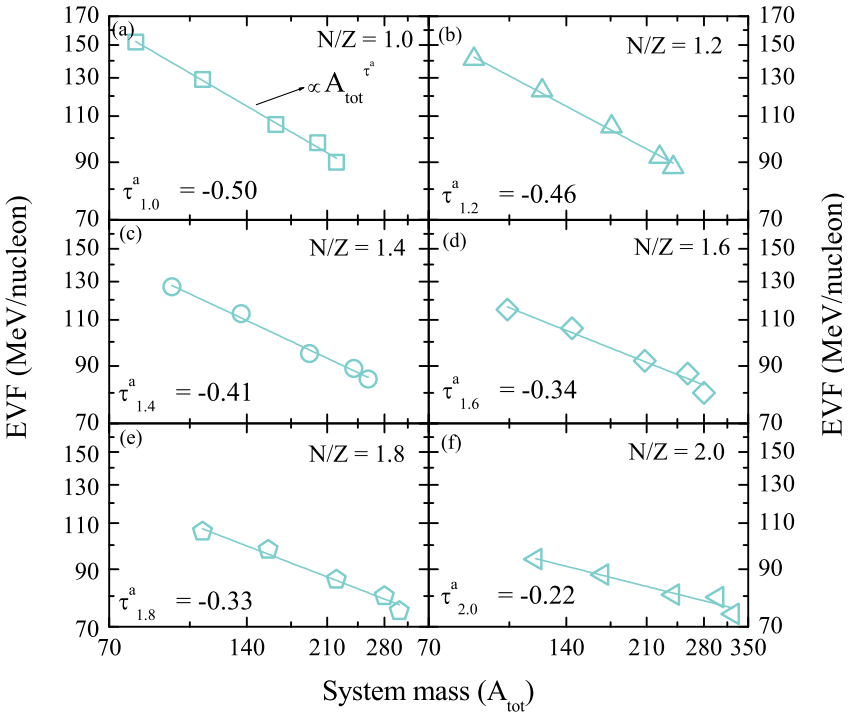

Figure 6. The EVF as a function of the combined reacting mass for various N/Z ratios at $\hat{b}$ = 0.4 - 0.6. The lines are power law fits $\propto A^{\tau^a}$.

also, to see the effect of the symmetry energy, we reduce its strength to zero and calculate the EVF for two extreme mass systems of the Ca+Ca and Xe+Xe series. The results are displayed in Fig. 5 (open symbols). The top, middle and bottom panels represent the results for $\hat{b}$ = 0.2 - 0.4, 0.4 - 0.6 and 0.6 - 0.8, respectively. From the figure, we see that the EVF increases for both of the masses on reducing the strength of the symmetry potential whereas the slope of the N/Z dependence of the EVF decreases drastically for both of the systems. The magnitude of the slopes are 11 (1), 21 (2) and 100 (2) for the reactions of Ca+Ca (Xe+Xe) at $\hat{b}$ = 0.2 - 0.4, 0.4 - 0.6 and 0.6 - 0.8, respectively. From the figure, we also note that the percentage change ($\triangle$m (%)= $|\frac{m^{symm.\ off} - m}{m}| \times 100$) in the slope for Ca (Xe) series is 67 (93) at $\hat{b}$ = 0.2 - 0.4 whereas it is 64 (89) at $\hat{b}$ = 0.4 - 0.6.

In Figs. 6 and 7, we display the system size dependence of the EVF for various N/Z ratios varying from 1.0 to 2.0 for $\hat{b}$ = 0.4 - 0.6 and $\hat{b}$ = 0.6 - 0.8, respectively. The various symbols have the same meaning as in Fig. 3. From Figs. 6 and 7, we see that the EVF follows a power law behavior ($\propto A_{tot}^{\tau^a}$) with system size at both collision geometries. The power law parameter τ^a is -0.50 (-1.03), -0.46 (-0.87), -0.41 (-0.81), -0.34 (-0.72), -0.33 (-0.63), and -0.22 (-0.59), respectively, for N/Z ratios of

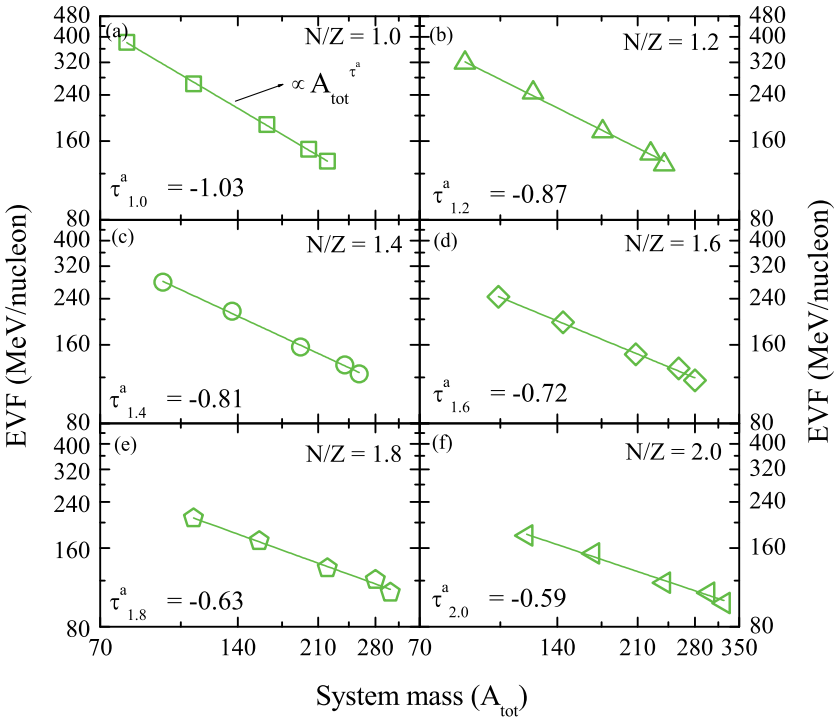

Figure 7. Same as Fig. 6, but for $\hat{b}$ = 0.6 - 0.8.

1.0, 1.2, 1.4, 1.6, 1.8, and 2.0 at $\hat{b}$ = 0.4 - 0.6 (0.6 - 0.8). We find that the power law parameter goes on decreasing as we move towards asymmetric nuclear matter (higher N/Z). This is due to the fact that for higher N/Z ratios, the effect of the symmetry energy is larger in lighter masses and thus decreases the EVF by a larger magnitude in lighter masses that results in a smaller slope for a higher N/Z ratio. Moreover, we also find that the slope parameter increases for peripheral collisions. This increase in the value of the slope parameter is due to the fact that the EVF for lighter systems (like Ca+Ca) changes drastically with impact parameter but the change of the EVF with impact parameter in heavier masses is smaller [20], which results in the increase of the slope parameter for peripheral collision geometries.

3 Summary

We studied the N/Z dependence of the energy of vanishing flow for various isotopic series of Ca+Ca, Ni+Ni, Zr+Zr, Sn+Sn and Xe+Xe reactions for the whole range of collision geometry from central to peripheral collisions. Our investigations revealed that the N/Z dependence of the energy of vanishing

flow is sensitive to the symmetry energy. Moreover, the sensitivity of the symmetry energy towards the behavior of the energy of vanishing flow with neutron content is found to be much higher for heavier masses, indicating that the N/Z dependence of the energy of vanishing flow of heavier systems can act as a good probe to constrain the symmetry energy in the supra-saturation region. The energy of vanishing flow followed a power law behavior with system size for colliding pairs far from the β-stability line, though the power law factor varies with the neutron-content of the colliding pairs.

References

[1] R. K. Puri and R. K. Gupta, Phys. Rev. C **45**, 1837 (1992); R. K. Puri, M. M. Sharma and R. K. Gupta, Eur. Phys. J A **3**, 277 (1998); R. K. Puri and N. Dhiman, *ibid*. A **23**, 429 (2005); I. Dutt and R. K. Puri, Phys. Rev. C **81**, 047601 (2010); *ibid*. C **81**, 044615 (2010); *ibid*. C **81**, 064608 (2010); *ibid*. C **81**, 064609 (2010).

[2] R. K. Puri *et al*., Nucl. Phys. A **575**, 733 (1994); D. T. Khoa *et al*., *ibid*. A **548**, 102 (1994).

[3] C. L. Jiang, B. B. Back, H. Esbensen, R. V. F. Janssens, and K. E. Rehm, Phys. Rev. C **73**, 014613 (2006); N. G. Nicolis, Eur. Phys. J. A **21**, 265 (2004); L. C. Vaz *et al*., Phys. Rep. **69**, 373 (1981).

[4] C. Sturm *et al*., Phys. Rev. Lett. **86**, 39 (2001); C. Hartnack, J. Jaenicke, L. Shen, H. Stöcker, and J. Aichelin, Nucl. Phys. **A580**, 643 (1994).

[5] J. Singh *et al*., Phys. Rev. C **65**, 024602 (2002); J. Singh, R. K. Puri and J. Aichelin, Phys. Lett. B **519**, 46 (2001); D. Sisan *et al*., Phys. Rev. C **63**, 027602 (2001).

[6] A. D. Sood and R. K. Puri, Phys. Rev C **70**, 034611 (2004); A. D. Sood, R. K. Puri and J. Aichelin, Phys. Lett. B **594**, 260 (2004); R. Chugh and R. K. Puri, Phys. Rev. C **82**, 014603 (2010).

[7] C. A. Ogilvie *et al*., Phys. Rev. C **40**, 2592 (1989); B. Blättel, V. Koch, A. Lang, K. Weber, W. Cassing, and U. Mosel, *ibid*. C **43**, 2728 (1991.

[8] Q. Pan and P. Danielewicz, Phys. Rev. Lett. **70**, 2062 (1993); J. Lukasik *et al*., Phys. Lett. **B608**, 223 (2005); V. Ramillien *et al.*, Nucl. Phys. **A587**, 802 (1995).

[9] Y. Zhang and Z. Li, Phys. Rev. C **74**, 014602 (2006); B. Hong *et al*., Phys. Rev. C **66**, 034901 (2000); L. Scalone, M. Colonna, and M. Di Toro, Phys. Lett. **B461**, 9 (1999).

[10] D. Krofcheck *et al*., Phys. Rev. Lett. **63**, 2028 (1989).

[11] G. D. Westfall *et al*., Nucl. Phys. A **681**, 342c (2001); A. D. Sood and R. K. Puri, Phys. Rev. C **73**, 067602 (2006); D. J. Magestro *et al*., Phys. Rev. C **61**, 021602(R) (2000); G. D. Westfall *et al*., Phys. Rev. Lett. **71**, 1986 (1993).

[12] B. A. Li, Phys. Rep. **464**, 113 (2008).

[13] W. Zhan *et al*., Int. J. Mod. Phys. E **15**, 1941 (2006); see, e.g. http://www.impcas.ac.cn/zhuye/en/htm/247.htm.

[14] See, e.g., http://www.gsi.de/en/research/fair.html; See, e.g., http://ganil-spiral2.eu/.

[15] Y. Yano, Nucl. Inst. Methods B **261**, 1009 (2007).

[16] B. A. Li, Z. Ren, C. M. Ko, and S. J. Yennello, Phys. Rev. Lett. **76**, 4492 (1996); C. Liewen, Z. Fengshou, and J. Genming, Phys. Rev. C **58**, 2283 (1998).

[17] S. Gautam and A. D. Sood, Phys. Rev. C **82**, 014604 (2010).

[18] S. Gautam *et al*., Phys. Rev. C **83**, 014603 (2011).

[19] C. Hartnack *et al*., Eur. Phys. J. A **1**, 151 (1998); S. Kaur and R. K. Puri, Phys. Rev. C **87**, 014620 (2013); R. Bansal, S. Gautam, R. K. Puri and J. Aichelin, *ibid*. C **87**, 061602(R) (2013); S. Kumar, S. Kumar and R. K. Puri, *ibid*. C **81**, 014601 (2010); *ibid*. C **81**, 014611 (2010).

[20] D. J. Magestro *et al*., Phys. Rev. C **62**, 041603(R) (2000).